

## Article

# Amphiphilic Alkylated Pectin Hydrogels for Enhanced Topical Delivery of Fusidic Acid: Formulation and In Vitro Investigation

Mohammad F. Bostanudin College of Pharmacy, Al Ain University, Abu Dhabi 112612, United Arab Emirates;  
mohammad.bostanudin@aau.ac.ae

**Abstract:** Hydrogels constructed of amphiphilically modified polysaccharides have attracted a lot of interest because of their potential to augment drug diffusion over the skin. This research describes the synthesis of amphiphilic alkylated pectin via glycidyl *tert*-butyl ether modification (alkylation degree 15.7%), which was characterized using spectroscopic and thermal analysis techniques and then formulated into hydrogels for the study of their potential in regulating fusidic acid diffusion topically. The hydrogels were formulated by the ionic interaction of negatively charged pectin and positively charged crosslinker CaCl<sub>2</sub>, with a reported fusidic acid loading degree of 93–95%. Hydrogels made of alkylated pectin showed a lower swelling percentage than that of native pectin, resulting in a slower fusidic acid release. The influence of pH on the swelling percentage and drug release was also investigated, with results revealing that greater pH enhanced swelling percentage and drug release. The in vitro interactions with HaCaT cells revealed negligible cytotoxicity under application-relevant settings. Utilizing Franz diffusion cells, the alkylated pectin hydrogels caused fusidic acid to penetrate the Strat-M<sup>®</sup> membrane at a 1.5-fold higher rate than the native pectin hydrogels. Overall, the in vitro results showed that alkylated pectin hydrogels have a lot of promise for topical distribution, which needs further investigation.

**Keywords:** pectin; polymer synthesis; hydrogel; topical



**Citation:** Bostanudin, M.F. Amphiphilic Alkylated Pectin Hydrogels for Enhanced Topical Delivery of Fusidic Acid: Formulation and In Vitro Investigation. *Sci. Pharm.* **2022**, *90*, 13. <https://doi.org/10.3390/scipharm90010013>

Academic Editor: Yogeshvar N. Kalia

Received: 28 December 2021

Accepted: 10 February 2022

Published: 14 February 2022

**Publisher's Note:** MDPI stays neutral with regard to jurisdictional claims in published maps and institutional affiliations.



**Copyright:** © 2022 by the author. Licensee MDPI, Basel, Switzerland. This article is an open access article distributed under the terms and conditions of the Creative Commons Attribution (CC BY) license (<https://creativecommons.org/licenses/by/4.0/>).

## 1. Introduction

Antibiotic resistance is a major healthcare issue that has been recognized as the second leading cause of mortality worldwide. The inefficiency of topical antibiotic therapy, characterized by poor skin penetration and local discomfort, has been linked to antibiotic resistance [1]. Effective absorption or penetration via the skin is hampered due to the presence of stratum corneum, which functions as an impedance to hydrophilic, ionized, and large therapeutic actives [2,3]. Numerous approaches have been explored to overcome this barrier, but unwanted side effects, most prominently skin irritation and insufficient permeability, remain challenges for effective topical administration [4,5].

Fusidic acid is a narrow-spectrum antibacterial drug derived from the fungus *Fusidium coccineum* that is most potent against Gram-positive bacteria, including *Staphylococcus*, *Streptococcus*, and *Corynebacterium* spp. [6]. Fusidic acid, which is commonly found in commercial cream and ointment products, has been reported to possess poor penetration and absorption into the skin and does not stay on the skin for long [7]. Hydrogels have been investigated and utilized extensively for various drug delivery systems, among which topical drug delivery is remarkable. Hydrogels are greatly hydrated formations made up of hydrophilic polymeric chains. Crosslinks produced between these chains through various forms of physical interactions or chemical bonding are responsible for their structural stability [8].

A wide range of polysaccharides has been investigated for use in the formation of hydrogels. Pectin, an anionic hydrophilic polysaccharide found in the plant cells' central

lamella and typically derived from the cell wall of apple pomace or citrus peel, was used as the starting material in this study [9,10]. Pectin is biocompatible, non-toxic, and non-antigenic, with two functionalities—carboxyl (-COOH) and hydroxyl groups (-OH)—that allow for a number of chemical modifications for use in numerous applications [11,12]. Well-known for its mucoadhesive property, pectin has been extensively deployed in a variety of drug delivery systems to deliver drugs topically across the skin. Pectin-based hydrogels have attracted a lot of interest due to their desirable qualities and significant potential not only in enhancing wound healing activity [13,14], but also in drug delivery of actives like rivastigmine and tetracycline [15,16]. A study that explored the use of a hydrogel system based on pectin nanoparticles in the topical administration of *Amblystoma mexicanum* protein found increased wound healing activity [17].

The use of amphiphilic polysaccharides to make hydrogels has the remarkable effect of potentially enhancing medicinal ingredient penetration through biological membranes [18]. Among the most common chemical modifications conducted on pectin, the incorporation of alkyl moieties affects the macromolecule hydrophilic-lipophilic balance, causing hydrophilic polysaccharides to become amphiphilic and, as a result, govern skin permeability [19,20]. A range of chemicals, including epoxide derivatives such as glycidyl *tert*-butyl ether (GTBE), can be used to add alkyl moieties to hydrophilic polysaccharides. Several studies employing amphiphilic-based polysaccharides in drug delivery have demonstrated the ability to augment the skin penetration of different actives [21,22].

Vindicated by the fact that amphiphilic materials can boost drug penetration topically, this study investigates the fabrication of amphiphilically modified pectin with glycidyl *tert*-butyl ether—a hydrophobic alkylglycerol—and its formulation into hydrogels for the topical delivery of fusidic acid. To the best of the author's knowledge, no literature has reported the feasibility of employing amphiphilically modified pectin hydrogels to improve fusidic acid transport through the skin. The synthesis and characterization of the amphiphilically modified pectin, along with its formulation into hydrogels, are reported. *In vitro* cytotoxicity (against immortalized human epidermal keratinocyte cells), drug release, and permeability investigations are also addressed.

## 2. Materials and Methods

### 2.1. Materials

Pectin (from citrus, 20–34% esterification, MW 17 kDa), glycidyl *tert*-butyl ether (GTBE), fusidic acid, sodium hydroxide (NaOH), phosphate-buffered saline (PBS), calcium chloride (CaCl<sub>2</sub>), and citrate-phosphate buffer (CPB) were acquired from Sigma-Aldrich (Buchs, SG, Switzerland). Strat-M<sup>®</sup> and dialysis membranes molecular weight cut-off (MWCO) 12–14 kDa were acquired from Merck Millipore (Burlington, MA, USA). Dulbecco's Modified Eagle's Medium (DMEM), trypsin-EDTA, and fetal calf serum (FCS) were acquired from Invitrogen Gibco (Carlsbad, California, USA). Hydrochloric acid (HCl), dichloromethane (DCM), and dimethyl sulfoxide (DMSO) were supplied by Merck Co. (Darmstadt, Hesse, Germany).

### 2.2. Synthesis of Alkylated Pectin Derivative

An aq. pectin solution (2 g; 10.3 mmol; 50 mL) was adjusted to pH 12 with NaOH (33% *w/v*) before being frozen for 2 days. After it was thawed, GTBE reagent (5.90 mL; 41.24 mmol) was carefully introduced under magnetic stirring, and the reaction was maintained for 4 h at 40 °C under an N<sub>2</sub> ambiance before being neutralized with HCl (10% *v/v*). The mixture was thoroughly washed (×3) with DCM to eliminate H<sub>2</sub>O-insoluble impurities prior to rotavaporation (Stuart RE-402, Bibby Sterilin Ltd., Stone, Staffordshire, UK) at 45 °C. The mixture was further purified by a 72-h dialysis (MWCO 12–14 kDa) against dH<sub>2</sub>O (10 L; 9 washes) to remove H<sub>2</sub>O-soluble impurities before being freeze-dried (Labfreez FD-10-MR<sup>®</sup>, Labfreez Co. Ltd., Haidian, Beijing, China).

### 2.3. Characterization of Alkylated Pectin Derivative

The alkylated pectin  $^1\text{H-NMR}$  spectra were recorded on a Bruker Ascend 700 spectrometer (Bruker, Karlsruhe, Germany; 700 MHz) and subsequently used to quantify the degree of alkylation (DA), which presented as the alkyl chain no. connected to 100 pectin molecules; 100% denotes that all four possible locations in a single sugar molecule were completely altered. The following Equation (1), derived from the peak integrals attributed to the end  $\text{CH}_3$  of the alkyl chain (1.1 ppm) and the H-1 anomeric proton (5.0 ppm), was used to quantify the DA:

$$DA (\%) = \frac{A \times 100}{3B} \quad (1)$$

where:

DA (%): degree of alkylation (the alkyl chains number connected to 100 pectin molecules),  
A: the alkyl chain end  $\text{CH}_3$  integral ( $\delta$  1.1 ppm), and  
B: the glucopyranosic ring anomeric proton integral ( $\delta$  5.0 ppm).

The FT-IR spectra were recorded on a Bruker Tensio-II infrared spectrometer mounted with a single reflection diamond ATR (Bruker, Ettlingen, Germany) from wavenumber  $4000\text{--}500\text{ cm}^{-1}$  range, and 32 scans were averaged at a resolution of  $4\text{ cm}^{-1}$ . Thermal analysis by differential scanning calorimetry (DSC) was performed at varying temperatures ( $-50$  to  $250\text{ }^\circ\text{C}$ ) on a NETZSCH DSC 214 Polyma (NETZSCH, Selb, Germany;  $10\text{ K min}^{-1}$  heating/cooling rate;  $40\text{ mL min}^{-1}$   $\text{N}_2$  flow rate).

### 2.4. Fabrication of Fusidic Acid-Loaded Hydrogels

A solution of glycerol (5% *w/w*; 6 mL) was added to an aq. pectin solution (2%; 30 mL) under magnetic stirring prior to gentle addition of fusidic acid solution in pH 8 buffer; the mixture was left stirring for 24 h. Following that, a  $\text{CaCl}_2$  solution (7% *w/w*) was added to the mixture to produce crosslinked hydrogels which were subsequently transferred to a petri dish and dried at  $25\text{ }^\circ\text{C}$  for 24 h on an orbital shaker. For comparison, hydrogels made of native pectin were also prepared following the same techniques.

The morphology of the hydrogels was studied utilizing scanning electron microscopy (SEM). The hydrogels ( $5\text{ mm}^2$ ) were lyophilized for 15 h before being deposited onto an aluminum stub. A thin gold alloy coating (vacuum sputter coater Q150RES; Quorum Technologies Ltd., Ashford, Kent, UK) was applied to the samples prior to visualization.

### 2.5. Swelling Studies

A dry hydrogel sample of either alkylated or native pectin (3 g) was carefully weighed (WD) and submerged in either a pH 4 or 6 buffered solution to investigate the swelling behaviors. Following 2 h of incubation, the sample was withdrawn from the solution, the excessive water was extracted using filter paper, and the sample was weighed (WS). The weight increase (WI) was computed using Equation (2):

$$WI (\%) = \frac{WS - WD}{WD} \times 100 \quad (2)$$

### 2.6. Drug Loading and Release Studies

To investigate hydrogel drug loading ability, a blank hydrogel sample (either alkylated or native pectin) was formulated (without drug) following the techniques outlined in Section 2.4. Following drying, a dry blank hydrogel sample (4 mg) was added to a pH 8 buffered fusidic acid solution (15 mg/mL; 2 mL) in a test tube. The test tube was shaken using an orbital shaker at  $25\text{ }^\circ\text{C}$  and the concentration of fusidic acid in the solution was detected over time by a UV spectrophotometer (Perkin-Elmer Lambda 25, Perkin-Elmer Ltd., Beaconsfield, Buckinghamshire, UK) at 285 nm.

The drug release profiles of the hydrogels were assessed according to a methodology outlined in literature [23], as follows: fusidic acid-loaded hydrogel disks were placed in vials consisting of either pH 4 or 6 buffer (40 mL) and agitated in an orbital shaker at  $25\text{ }^\circ\text{C}$ .

The amount of drug released into the solution was detected using a UV spectrophotometer set to 285 nm.

### 2.7. Cytotoxicity Assay

Immortalized human epidermal keratinocyte (HaCaT) cell line was acquired from Cell Lines Service (Eppelheim, Baden Württemberg, Germany) and cultivated in DMEM (100  $\mu$ L) at 37 °C under a humidified 5% CO<sub>2</sub> ambiance. Either a native (2 mg) or alkylated pectin hydrogel sample (2–5 mg) was cultured with effluent HaCaT cells (seeding  $6 \times 10^4$ /well) for 24 h at 37 °C. The cells were then treated with MTT solvent (50  $\mu$ L; 10 mg/mL) and cultured for a further 4 h before getting treated with DMSO (50  $\mu$ L). The plate was evaluated using a Multiskan GO microplate reader (set to 570 nm; Thermo Fisher Scientific, Waltham, MA, USA), with PBS serving as a control.

### 2.8. In Vitro Permeability Studies

Franz<sup>TM</sup> diffusion cells (PermeGear Inc., Hellertown, PA, USA) with Strat-M<sup>®</sup> membranes fixed between the receiver and donor chambers (diffusion area 1.77 cm<sup>2</sup>) were used in this study. The receptor chamber was supplied with a pH 4 buffer and maintained at 37 °C by means of a surrounding jacket under magnetic agitation. Either native or alkylated pectin hydrogel sample (300 mg) was added to the donor compartment. At regular intervals up to 8 h, samples (500  $\mu$ L) were obtained from the receptor compartment, and similar fresh pH 4 buffer was promptly re-introduced to maintain sink conditions. At 285 nm, the samples were spectrophotometrically examined. Permeation profile curves were constructed by graphing the total quantity permeated ( $\mu$ g/cm<sup>2</sup>) vs. time (h). The linear component gradient of the graph was also employed to estimate the steady-state flux (*J*).

### 2.9. Data Statistical Analysis

SPSS software (v.22, SPSS Inc., Chicago, IL, USA) was used to do the statistical analysis. Unless otherwise specified, a minimum of three measures ( $n = 3$ ) were taken and the statistical significance was evaluated by means of one-way analysis of variance (ANOVA) with  $p \leq 0.05$ . The results were tabulated as mean  $\pm$  standard deviation (SD).

## 3. Results and Discussion

Pectin was effectively alkylated using glycidyl *tert*-butyl ether (GTBE) in an excessively NaOH alkaline environment, yielding alkylated pectin (Figure 1) with altered characteristics (yield 87–91%). The alkali metal hydroxide, NaOH, catalyzed the synthesis—which followed the nucleophilic substitution S<sub>N</sub>2 reaction—to produce a strong nucleophile and break the epoxide ring before connecting the alkyl chain. The alkyl chain attached to the pectin backbone is anticipated to be non-specific, and it might have happened at both the C-6 carboxylate and hydroxyl groups [24].

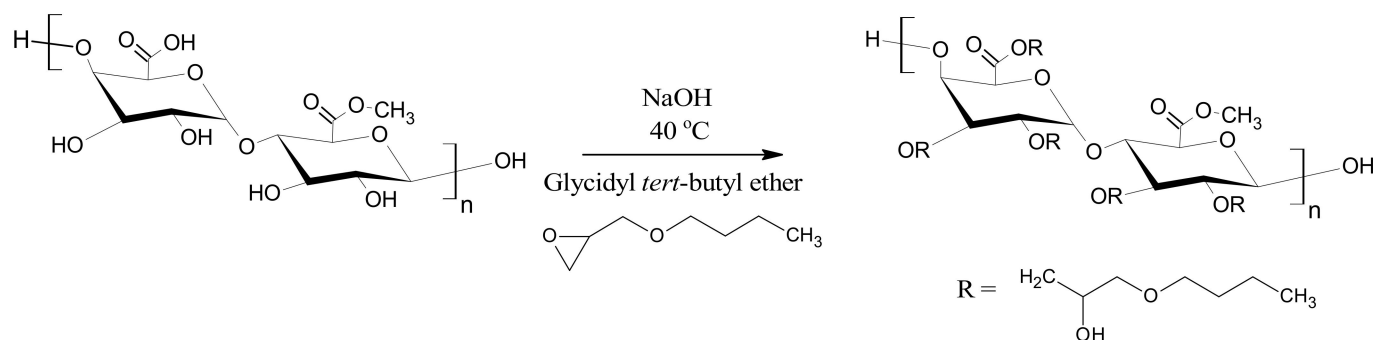


**Figure 1.** An illustration of the alkylated pectin synthesis.

The FTIR analysis of alkylated pectin was used to identify the spectroscopic alterations brought by the glycidyl *tert*-butyl ether modification, and the findings were compared to the native pectin. In general, the principal characteristic peaks of alkylated pectin were identical to those of native pectin. The extensive and intense absorption band at  $3329\text{ cm}^{-1}$  (seen in the spectra of both native and alkylated pectin, Figure 2) can be ascribed to -OH stretching absorption because of hydrogen bonding found in the galacturonic acid sub-units [25]. The bands at  $2921\text{--}2884\text{ cm}^{-1}$  are caused by -CH vibrations [11]. The absorption band at  $1764\text{ cm}^{-1}$  is caused by the carbonyl group of the methyl ester (-COOCH<sub>3</sub>) and unionized carboxylic acid (-COOH), whereas the band at  $1648\text{ cm}^{-1}$  is caused by the asymmetric stretching band of the carboxylate ion (COO<sup>-</sup>) [26]. Due to the formation of more linear ether (COC) links and the addition of more methyl groups, alkylation with GTBE increased the strength of the ether band ( $1149\text{--}1020\text{ cm}^{-1}$ ) as well as the -CH vibration bands ( $2921\text{--}2884\text{ cm}^{-1}$ ) [27–29].

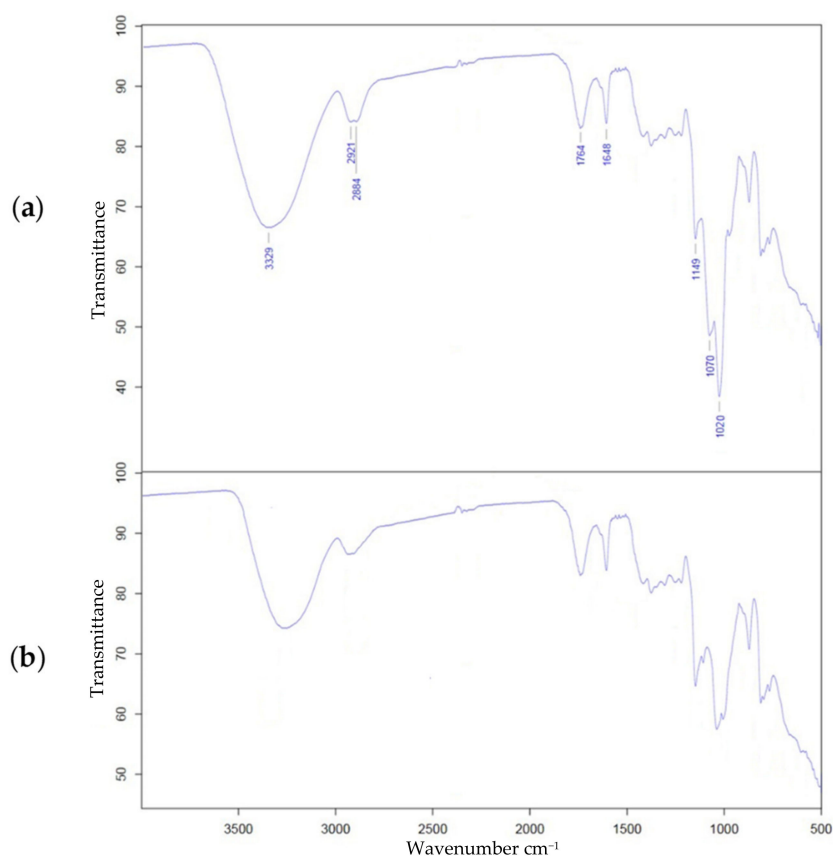


**Figure 2.** Typical FTIR-ATR spectra of alkylated (a) and native (b) pectin.

The synthesis was also validated using NMR spectroscopy. The H-1 anomeric proton was detected in the <sup>1</sup>H-NMR spectrum (Figure 3), and the peaks were allocated as follows:  $\delta$  5.0 ppm for the H-1 anomeric proton,  $\delta$  4.7 ppm for the free carboxylate group H-5 proton,  $\delta$  4.3 ppm for the H-4 proton,  $\delta$  3.9 ppm for the H-3 proton, and  $\delta$  3.7 ppm for the methoxy H-2 proton [30,31]. Peaks at  $\delta$  1.1, 1.4, and 1.6 ppm appeared after alkylation with glycidyl *tert*-butyl ether, suggesting the existence of new alkyl chains and proving reaction success [32]. The degree of alkylation (DA) was quantified from the <sup>1</sup>H-NMR spectra employing Equation (1), providing a DA of 15.7%.

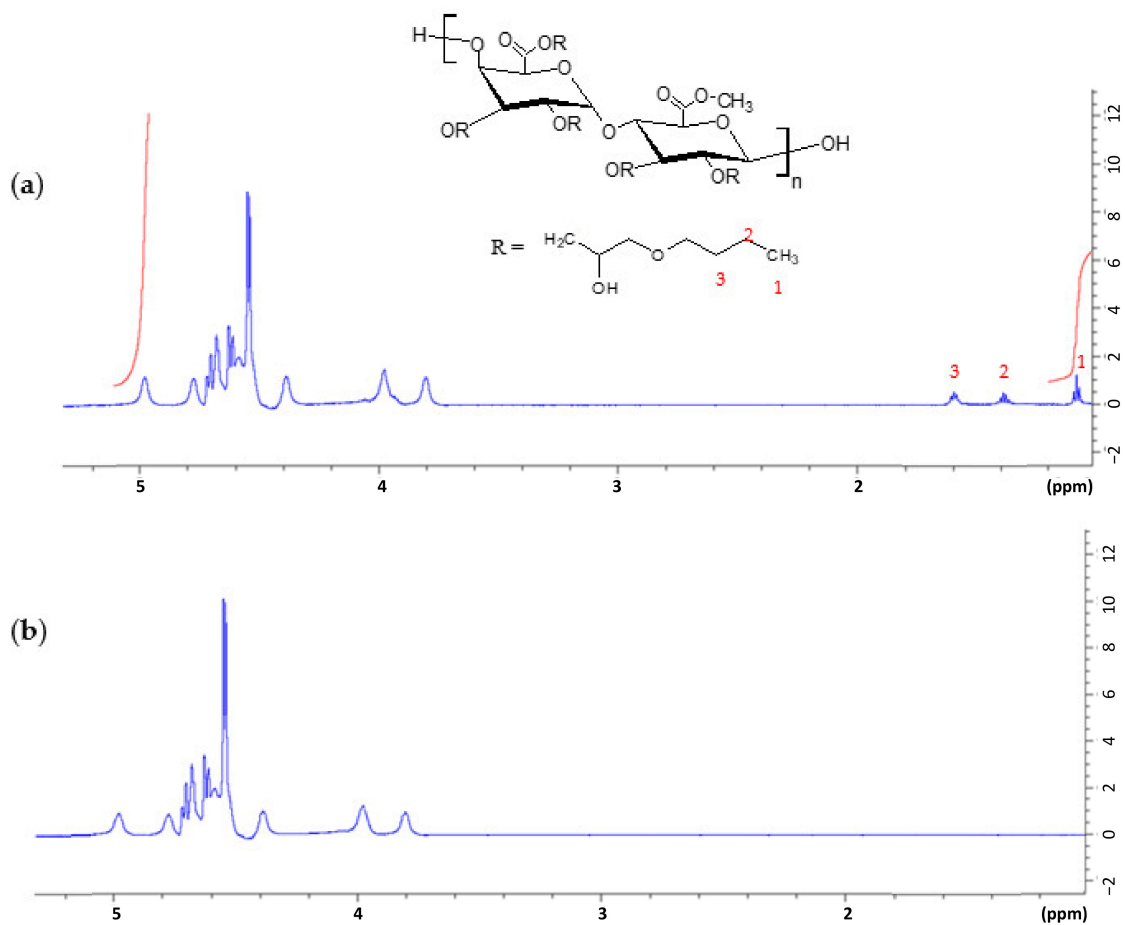


**Figure 3.** Typical <sup>1</sup>H-NMR spectrum of alkylated (a) and native (b) pectin.

Figure 4 depicts the results of a thermal examination using DSC to demonstrate how physical features of pectin vary as temperature rises. The natural pectin glass transition temperature ( $T_g$ ) was found to be around 35.7 °C, which is consistent with the literature [33]. The  $T_g$  of the alkylated pectin, on the other hand, climbed to around 40.3 °C after the chemical alteration. The addition of the alkyl chain to pectin bulked up the molecular structure and decreased mobility. Because of the enhanced hydrophobicity in the alkylated pectin, bound  $\text{H}_2\text{O}$  was eliminated, resulting in a higher  $T_g$  in the alkylated pectin; bound  $\text{H}_2\text{O}$  functions as a plasticizer, boosting chain mobility and lowering intermolecular forces [34,35].

The three-dimensional structure of hydrogels was prepared based on the ionic interaction between pectin and the  $\text{CaCl}_2$  crosslinker. Glycerol was added during the formulation process to improve hydrogel consistency, hardness, and cohesiveness [36]. To explore the real structures, the hydrogel morphology was visualized by SEM, and the images are displayed in Figure 5. Based on the results, the hydrogels possessed a porous structure, with native pectin hydrogels showing more porosity than the alkylated pectin hydrogels. This is perhaps due to a decrease in the swelling degree of the amphiphilic alkylated hydrogels, which inhibits the opening of the pores [37].

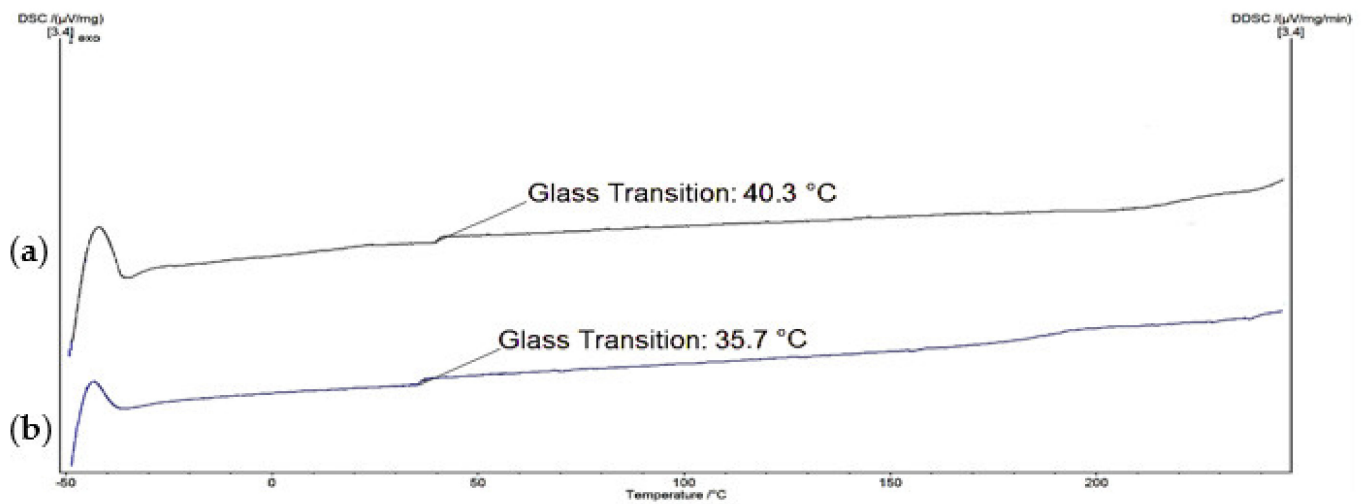


Figure 4. Typical DSC thermograms of alkylated (a) and native (b) pectin.

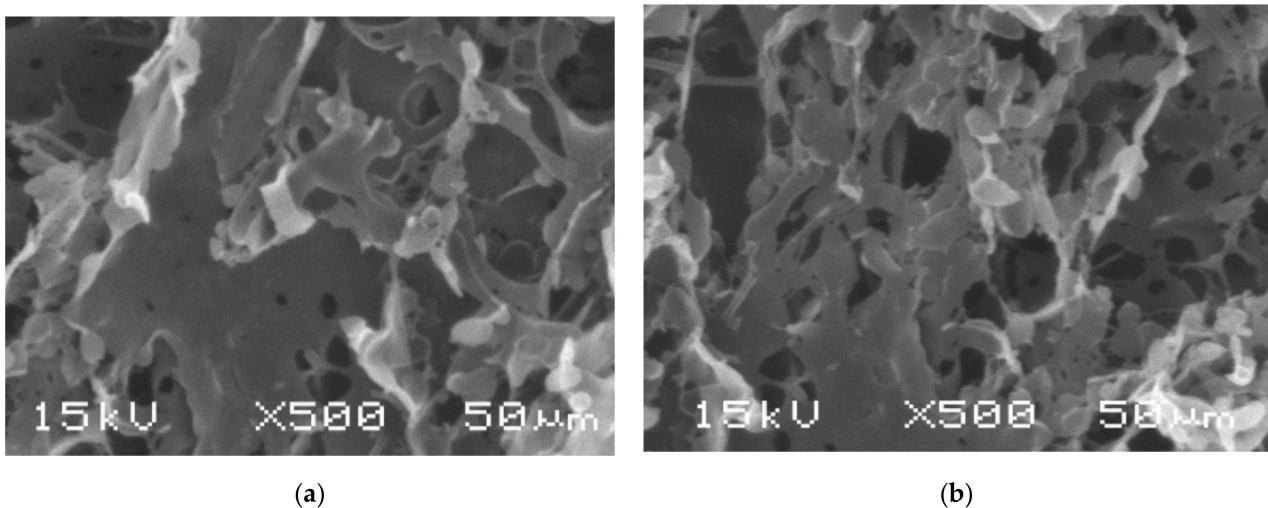
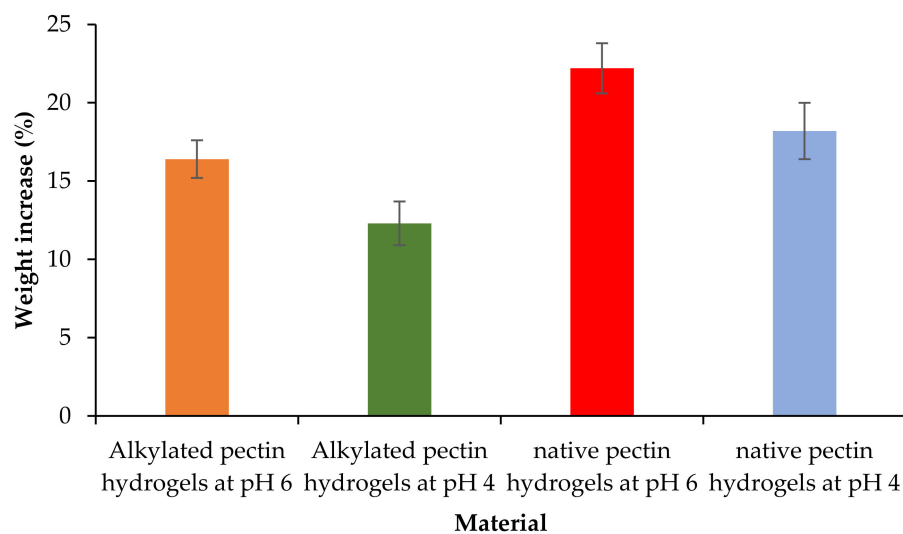


Figure 5. SEM micrographs of lyophilized alkylated (a) and native (b) pectin hydrogels (Bar: 50 μm).

Figure 6 displays the weight increase (%), which has elevated with the rising pH of the medium. Due to the hydrophilic nature of hydrogels, the swelling behaviors of the hydrogels can be expressed as weight increase (%) following the incorporation of water into the dry hydrogels [38,39]. The weight difference/increase between the swollen and dry hydrogels was calculated using Equation (2) to represent the swelling percentage of the hydrogels; the larger the weight increase (%), the higher the swelling percentage. As the medium pH was higher than the pKa of pectin (ca. 3.5), increasing negatively charged ions—due to ionization of carboxylic groups—in the pectin structure repulsed each other, resulting in wider gaps and porous structure [40,41]. As a result, by accessing this porous cross-linked structure, water may now interact with the hydrophilic polysaccharide and expand the hydrogels more quickly and effectively. When the swelling percentage rises, the structure of hydrogels softens. The existence of cross-links, however, limits further deformation of hydrogels, resulting in an osmotic pressure balance [42,43].



**Figure 6.** Swelling properties of pectin-based hydrogels following a 2-h incubation at different pH conditions ( $n = 3$ ;  $\pm$  SD).

In general, the alkylated pectin hydrogels showed a lower swelling percentage than the native pectin. This might be due to the fact that the alkylated pectin structure has a lesser number of accessible carboxylic groups since some of them may have been alkylated. The swelling behaviors of hydrogels are also influenced by the hydrophilic-hydrophobic balance of the polysaccharide. Polysaccharides containing more hydrophobic groups—in this case alkylated pectin—will have reduced interaction with water, hence preventing the hydrogels from further swelling. The presence of hydrophobic moieties also reduces the pH responsiveness of the hydrogels [44].

The hydrogel preparation and loading of fusidic acid into the hydrogels were done at pH 8 in order to maximize the loading degree since the carboxyl groups of pectin ionize better at high pH. The loading degree for hydrogels constructed of either alkylated pectin or native pectin was found comparable with values of around 93–95%. Due to the fact that skin pH ranges between 4 and 6, the release behavior of fusidic acid from the hydrogels was examined in media of those two distinct pH conditions. According to Figure 7, fusidic acid release increased over time in both media, with a slower release documented in the pH 4 medium as opposed to the pH 6 medium. Pectin, with pKa of ca. 3.5, has a decreased carboxyl group ionization rate in pH 4 medium, resulting in less swelling and small pore size. As a result, drug diffusion through the matrix of the hydrogels was slow. Conversely, it is also obvious that the hydrogels with a high swelling percentage generate quicker drug release owing to the repulsion of the internal polymer chains and the high porosity of the hydrogel structure [45]. Furthermore, alkylated pectin hydrogels with hydrophobic alkyl chains also release drugs at a slower rate than hydrophilic native hydrogels. This is perhaps due to a low swelling percentage, small pore size, and lack of water uptake, which is in accordance with the literature [46].

An MTT assay was deployed to test the hydrogel cytotoxicity against HaCaT cells *in vitro*, with PBS acting as a control. The human epidermal keratinocyte (HaCaT) cell line was employed since it has been used as a surrogate for human keratinocytes in various studies [47,48]. To explore the effect of concentration on cytotoxicity, the alkylated pectin hydrogels were tested at various concentrations (ranging from 2 to 5 mg). In comparison to the PBS control, the alkylated pectin hydrogels demonstrated > 94% cell viability (Figure 8) throughout the whole range of concentrations tested; similarly, the native pectin hydrogels also displayed good cell survival throughout the trial. The lack of a substantial difference between the alkylated hydrogels, native pectin hydrogels, and the control suggests that the alkylation did not induce any potential hazards. The previous study has also demonstrated

that polysaccharides modified with comparable short-chain alkylglycerols are safe for use in a variety of biomedical applications [29,49].

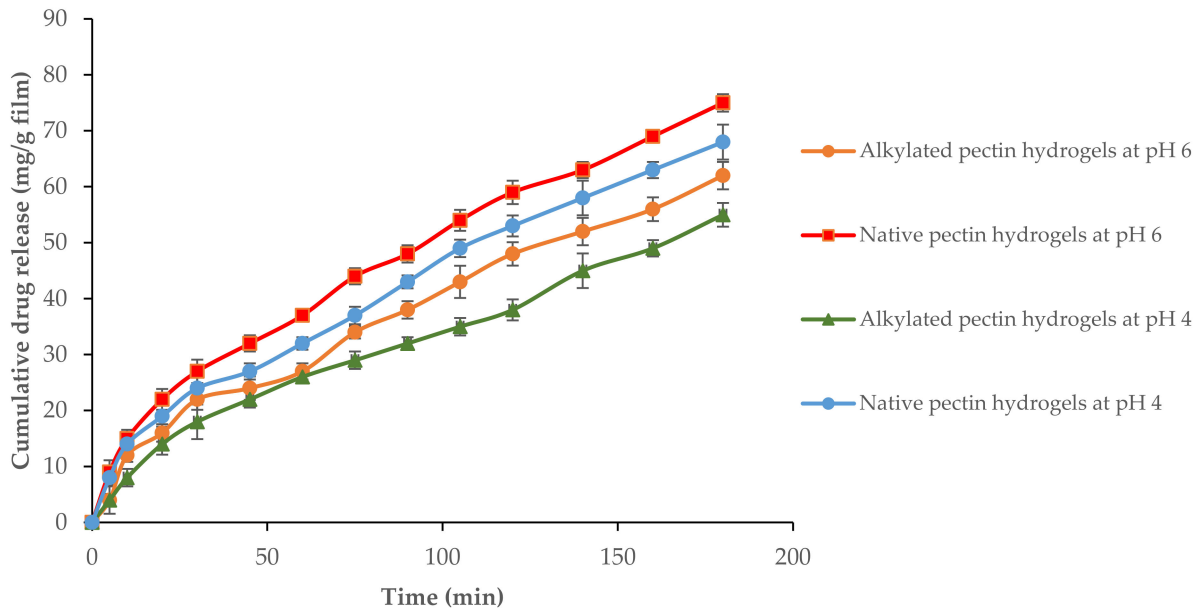


Figure 7. Fusidic acid release behavior from pectin-based hydrogels in either pH 4 or 6 buffer ( $n = 3$ ;  $\pm$  SD).

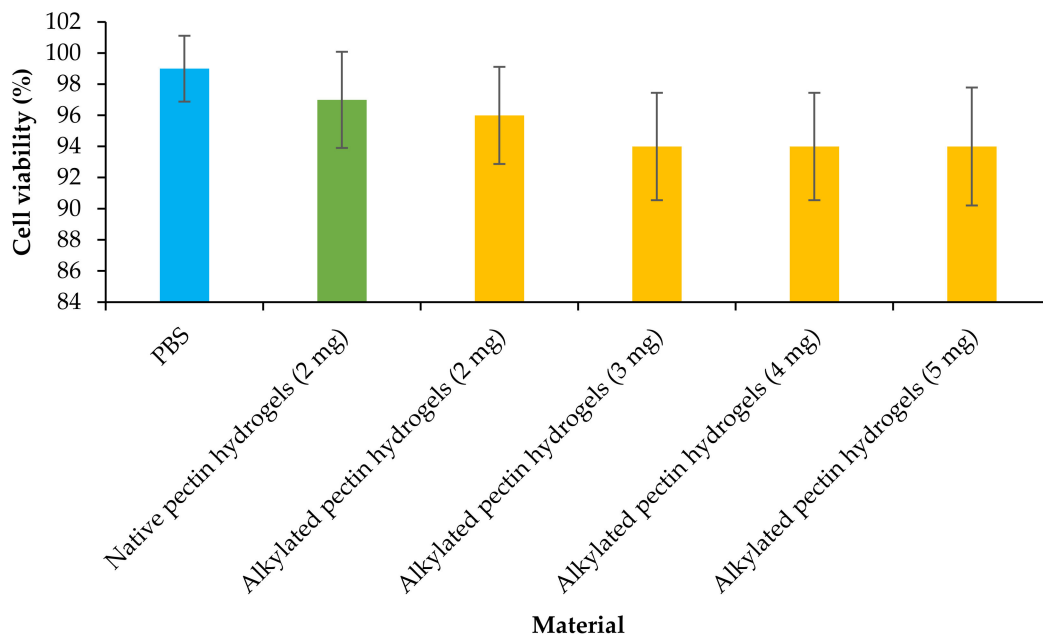
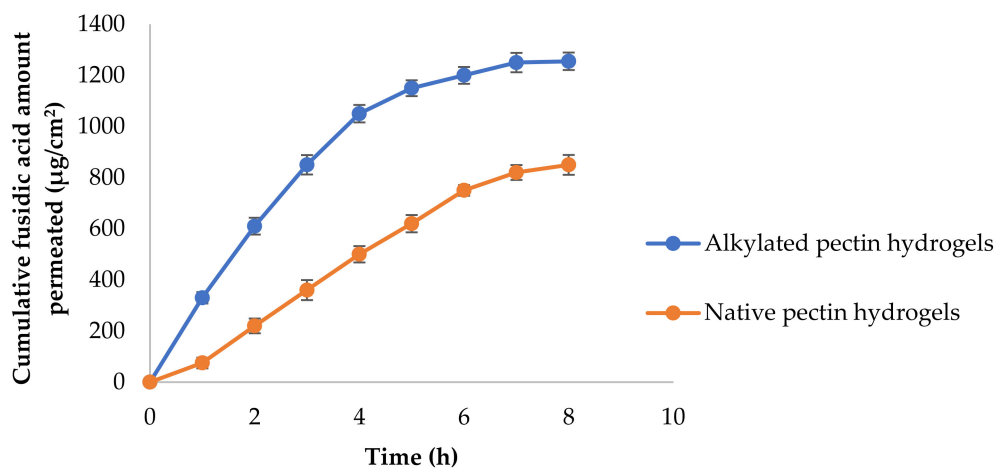


Figure 8. HaCaT cell viability analysis of pectin-based hydrogels ( $n = 3$ ;  $\pm$  SD).

Vertical Franz<sup>TM</sup> diffusion cells fixed with the Strat-M<sup>®</sup> membrane were deployed to examine in vitro the effect of the hydrogels in the permeability of fusidic acid across the skin (Figure 9). The Strat-M<sup>®</sup> membrane is thought to resemble comparable structural and functional qualities to those found in human skin [50,51]. At 8 h, the total fusidic acid amount permeated was  $1255.3 \pm 34.1 \mu\text{g}/\text{cm}^2$  and  $850.5 \pm 39.2 \mu\text{g}/\text{cm}^2$  for alkylated pectin and native pectin hydrogels, respectively. For alkylated pectin and native pectin hydrogels, the flux values ( $J$ ) were  $184.6 \pm 1.2 \text{ g}/\text{cm}^2 \text{ h}$  and  $125.8 \pm 1.1 \text{ g}/\text{cm}^2 \text{ h}$ , respectively. When compared to native pectin hydrogels, the penetration and flux of fusidic acid across the Strat-

M<sup>®</sup> membrane after 8 h was 1.5 times greater when formulated with amphiphilic alkylated pectin hydrogels. This is in accordance with our prior findings that reported higher drug permeation across skin models when formulated with amphiphilic polysaccharides [19,28]. Even though the exact mechanisms are obscure, it is possible that the amphiphilic alkylated pectin loosens the tight lipid packing and lowers barrier resistance, allowing more solute to pass through the skin [52].



**Figure 9.** Fusidic acid permeation through Strat-M<sup>®</sup> membrane ( $n = 3$ ;  $\pm$  SD).

#### 4. Conclusions

Alkylated pectin was successfully prepared by alkylation with glycidyl *tert*-butyl ether (DA 15.7%), then characterized employing spectroscopic and thermal analytical techniques before being formulated into hydrogels via the cross-linking technique. With a reported fusidic acid loading degree of 93–95%, the alkylated pectin hydrogels showed a lower swelling percentage and slower drug release than the native pectin hydrogels. The effect of medium pH was found to be directly proportional to swelling percentage and drug release. The cytotoxicity assay indicated negligible toxicity, and the produced alkylated pectin hydrogels caused fusidic acid to penetrate the Strat-M<sup>®</sup> membrane 1.5-fold better than the native pectin hydrogels *in vitro*. Finally, the findings demonstrated that alkylated pectin-based hydrogels offered adequate properties to warrant further investigation and optimization of their prospects for use in topical drug delivery.

**Funding:** This research was funded by Al Ain University (UAE) and University of Cyberjaya (Malaysia).

**Institutional Review Board Statement:** Not applicable.

**Informed Consent Statement:** Not applicable.

**Data Availability Statement:** Raw data required to reproduce these findings can be shared upon request.

**Acknowledgments:** Author would like to acknowledge Al Ain University (UAE) and University of Cyberjaya (Malaysia) for supporting the study.

**Conflicts of Interest:** The author declares no conflict of interest.

#### References

- Guo, Y.; Song, G.; Sun, M.; Wang, J.; Wang, Y. Prevalence and therapies of antibiotic-resistance in *Staphylococcus aureus*. *Front. Cell. Infect. Microbiol.* **2020**, *10*, 107. [[CrossRef](#)] [[PubMed](#)]
- Mercuri, M.; Fernandez Rivas, D. Challenges and opportunities for small volumes delivery into the skin. *Biomicrofluidics* **2021**, *15*, 11301. [[CrossRef](#)] [[PubMed](#)]
- Puri, A.; Murnane, K.S.; Blough, B.E.; Banga, A.K. Effects of chemical and physical enhancement techniques on transdermal delivery of 3-fluoroamphetamine hydrochloride. *Int. J. Pharm.* **2017**, *528*, 452–462. [[CrossRef](#)] [[PubMed](#)]

4. Haque, T.; Talukder, M.M.U. Chemical enhancer: A simplistic way to modulate barrier function of the stratum corneum. *Adv. Pharm. Bull.* **2018**, *8*, 169–179. [[CrossRef](#)]
5. Alkilani, A.Z.; McCrudden, M.T.C.; Donnelly, R.F. Transdermal drug delivery: Innovative pharmaceutical developments based on disruption of the barrier properties of the stratum corneum. *Pharmaceutics* **2015**, *7*, 438–470. [[CrossRef](#)]
6. Godtfredsen, W.O.; Jahnsen, S.; Lorck, H.; Roholt, K.; Tybring, L. Fusidic acid: A new antibiotic. *Nature* **1962**, *193*, 987. [[CrossRef](#)]
7. Eid, A.M.; Istateyeh, I.; Salhi, N.; Istateyeh, T. Antibacterial activity of Fusidic acid and sodium Fusidate nanoparticles incorporated in pine oil Nanoemulgel. *Int. J. Nanomed.* **2019**, *14*, 9411. [[CrossRef](#)]
8. Neves, S.C.; Gomes, D.B.; Sousa, A.; Bidarra, S.J.; Petrini, P.; Moroni, L.; Barrias, C.C.; Granja, P.L. Biofunctionalized pectin hydrogels as 3D cellular microenvironments. *J. Mater. Chem. B* **2015**, *3*, 2096–2108. [[CrossRef](#)]
9. Zdunek, A.; Pieczywek, P.M.; Cybulska, J. The primary, secondary, and structures of higher levels of pectin polysaccharides. *Compr. Rev. Food Sci. Food Saf.* **2021**, *20*, 1101–1117. [[CrossRef](#)]
10. Lal, A.M.N.; Prince, M.V.; Kothakota, A.; Pandiselvam, R.; Thirumdas, R.; Mahanti, N.K.; Sreeja, R. Pulsed electric field combined with microwave-assisted extraction of pectin polysaccharide from jackfruit waste. *Innov. Food Sci. Emerg. Technol.* **2021**, *74*, 102844. [[CrossRef](#)]
11. Bostanudin, M.F.; Arafat, M.; Sarfraz, M.; Górecki, D.C.; Barbu, E. Butylglyceryl pectin nanoparticles: Synthesis, formulation and characterization. *Polymers* **2019**, *11*, 789. [[CrossRef](#)]
12. Zhang, G.; Zheng, C.; Huang, B.; Fei, P. Preparation of acylated pectin with gallic acid through enzymatic method and their emulsifying properties, antioxidation activities and antibacterial activities. *Int. J. Biol. Macromol.* **2020**, *165*, 198–204. [[CrossRef](#)]
13. Kocaaga, B.; Kurkcuglu, O.; Tatlier, M.; Batirel, S.; Guner, F.S. Low-methoxyl pectin–zeolite hydrogels controlling drug release promote in vitro wound healing. *J. Appl. Polym. Sci.* **2019**, *136*, 47640. [[CrossRef](#)]
14. Li, D.; Wang, S.; Meng, Y.; Li, J.; Li, J. An injectable, self-healing hydrogel system from oxidized pectin/chitosan/ $\gamma$ -Fe<sub>2</sub>O<sub>3</sub>. *Int. J. Biol. Macromol.* **2020**, *164*, 4566–4574. [[CrossRef](#)]
15. Patil, S.B.; Inamdar, S.Z.; Reddy, K.R.; Raghu, A.V.; Akamanchi, K.G.; Inamadar, A.C.; Das, K.K.; Kulkarni, R.V. Functionally tailored electro-sensitive poly (acrylamide)-g-pectin copolymer hydrogel for transdermal drug delivery application: Synthesis, characterization, in-vitro and ex-vivo evaluation. *Drug Deliv. Lett.* **2020**, *10*, 185–196. [[CrossRef](#)]
16. Moghaddam, R.H.; Dadfarnia, S.; Shabani, A.M.H.; Moghaddam, Z.H.; Tavakol, M. Electron beam irradiation synthesis of porous and non-porous pectin based hydrogels for a tetracycline drug delivery system. *Mater. Sci. Eng. C* **2019**, *102*, 391–404. [[CrossRef](#)]
17. Oveissi, F.; Tavakoli, N.; Minaiyan, M.; Mofid, M.R.; Taheri, A. Alginate hydrogel enriched with *Ambystoma mexicanum* epidermal lipoxigenase-loaded pectin nanoparticles for enhanced wound healing. *J. Biomater. Appl.* **2020**, *34*, 1171–1187. [[CrossRef](#)]
18. Chang, H.; Li, C.; Huang, R.; Su, R.; Qi, W.; He, Z. Amphiphilic hydrogels for biomedical applications. *J. Mater. Chem. B* **2019**, *7*, 2899–2910. [[CrossRef](#)]
19. Bostanudin, M.F.; Barbu, E.; Liew, K. Bin Hydrophobically Grafted Pullulan Nanocarriers for Percutaneous Delivery: Preparation and Preliminary In Vitro Characterisation. *Polymers* **2021**, *13*, 2852. [[CrossRef](#)]
20. Li, S.; Xiong, Q.; Lai, X.; Li, X.; Wan, M.; Zhang, J.; Yan, Y.; Cao, M.; Lu, L.; Guan, J.; et al. Molecular Modification of Polysaccharides and Resulting Bioactivities. *Compr. Rev. Food Sci. Food Saf.* **2016**, *15*, 237–250. [[CrossRef](#)]
21. Aditya, A.; Chattopadhyay, S.; Gupta, N.; Alam, S.; Veedu, A.P.; Pal, M.; Singh, A.; Santhiya, D.; Ansari, K.M.; Ganguli, M. ZnO nanoparticles modified with an amphipathic peptide show improved photoprotection in skin. *ACS Appl. Mater. Interfaces* **2018**, *11*, 56–72. [[CrossRef](#)] [[PubMed](#)]
22. Zhao, Y.-C.; Zheng, H.-L.; Wang, X.-R.; Zheng, X.-L.; Chen, Y.; Fei, W.-D.; Zheng, Y.-Q.; Wang, W.-X.; Zheng, C.-H. Enhanced percutaneous delivery of methotrexate using micelles prepared with novel cationic amphipathic material. *Int. J. Nanomed.* **2020**, *15*, 3539. [[CrossRef](#)] [[PubMed](#)]
23. Rodoplu, S.; Celik, B.E.; Kocaaga, B.; Ozturk, C.; Batirel, S.; Turan, D.; Guner, F.S. Dual effect of procaine-loaded pectin hydrogels: Pain management and in vitro wound healing. *Polym. Bull.* **2021**, *78*, 2227–2250. [[CrossRef](#)]
24. Fan, L.; Cao, M.; Gao, S.; Wang, W.; Peng, K.; Tan, C.; Wen, F.; Tao, S.; Xie, W. Preparation and characterization of a quaternary ammonium derivative of pectin. *Carbohydr. Polym.* **2012**, *88*, 707–712. [[CrossRef](#)]
25. Arafat, M.; Fehelbom, K.M.; Sarfraz, M.K.; Bostanudin, M.F.; Sharif, Q.-A.; Esmaeil, A.; Hanbali, O.A.A.L.; Aburuz, S. Comparison between branded and generic furosemide 40 mg tablets using thermal gravimetric analysis and Fourier transform infrared spectroscopy. *J. Pharm. Bioallied Sci.* **2020**, *12*, 489. [[CrossRef](#)]
26. Demir, D.; Ceylan, S.; Göktürk, D.; Bölgen, N. Extraction of pectin from albedo of lemon peels for preparation of tissue engineering scaffolds. *Polym. Bull.* **2021**, *78*, 2211–2226. [[CrossRef](#)]
27. Panda, H. *Epoxy Resins Technology Handbook (Manufacturing Process, Synthesis, Epoxy Resin Adhesives and Epoxy Coatings)*; Asia Pacific Business Press Inc.: New Delhi, India, 2019; ISBN 8178331829.
28. Bostanudin, M.F.; Muhamad Noor, N.S.; Sahudin, S.; Mat Lazim, A.; Tan, S.F.; Sarker, M.Z.I. Investigations of amphiphilic butylglyceryl-functionalized dextran nanoparticles for topical delivery. *J. Appl. Polym. Sci.* **2021**, *138*, 50235. [[CrossRef](#)]
29. Bostanudin, M.F.; Salam, A.; Mahmood, A.; Arafat, M.; Kaharudin, A.N.; Sahudin, S.; Lazim, A.M.; Azfaralariff, A. Formulation and In-vitro Characterisation of Cross-linked Amphiphilic Guar Gum Nanocarriers for Percutaneous Delivery of Arbutin. *J. Pharm. Sci.* **2021**, *110*, 3907–3918. [[CrossRef](#)]

30. Kazemi, M.; Khodaiyan, F.; Hosseini, S.S. Utilization of food processing wastes of eggplant as a high potential pectin source and characterization of extracted pectin. *Food Chem.* **2019**, *294*, 339–346. [[CrossRef](#)]
31. Hosseini, S.S.; Khodaiyan, F.; Kazemi, M.; Najari, Z. Optimization and characterization of pectin extracted from sour orange peel by ultrasound assisted method. *Int. J. Biol. Macromol.* **2019**, *125*, 621–629. [[CrossRef](#)]
32. Toman, P.; Lien, C.-F.; Ahmad, Z.; Dietrich, S.; Smith, J.R.; An, Q.; Molnár, É.; Pilkington, G.J.; Górecki, D.C.; Tsiabouklis, J. Nanoparticles of alkylglyceryl-dextran-graft-poly (lactic acid) for drug delivery to the brain: Preparation and in vitro investigation. *Acta Biomater.* **2015**, *23*, 250–262. [[CrossRef](#)]
33. Iijima, M.; Nakamura, K.; Hatakeyama, T.; Hatakeyama, H. Phase transition of pectin with sorbed water. *Carbohydr. Polym.* **2000**, *41*, 101–106. [[CrossRef](#)]
34. Guidara, M.; Yaich, H.; Richel, A.; Blecker, C.; Boufi, S.; Attia, H.; Garna, H. Effects of extraction procedures and plasticizer concentration on the optical, thermal, structural and antioxidant properties of novel ulvan films. *Int. J. Biol. Macromol.* **2019**, *135*, 647–658. [[CrossRef](#)]
35. Li, H.; Yu, H.; Liu, Y.; Wang, Y.; Li, H.; Yu, J. The use of inulin, maltitol and lecithin as fat replacers and plasticizers in a model reduced-fat mozzarella cheese-like product. *J. Sci. Food Agric.* **2019**, *99*, 5586–5593. [[CrossRef](#)]
36. Szcześniak, M.; Grimling, B.; Meler, J.; Karolewicz, B. Application of chitosan in the formulation of dermatological hydrogels prepared on the basis of macromolecular compounds. *Prog. Chem. Appl. Chitin its Deriv.* **2018**, *23*, 179–184. [[CrossRef](#)]
37. Pekař, M. Hydrogels with micellar hydrophobic (nano) domains. *Front. Mater.* **2015**, *1*, 35. [[CrossRef](#)]
38. Sievers, J.; Sperlich, K.; Stahnke, T.; Kreiner, C.; Eickner, T.; Martin, H.; Guthoff, R.F.; Schünemann, M.; Bohn, S.; Stachs, O. Determination of hydrogel swelling factors by two established and a novel non-contact continuous method. *J. Appl. Polym. Sci.* **2021**, *138*, 50326. [[CrossRef](#)]
39. Kowalski, G.; Kijowska, K.; Witzak, M.; Kuterasiński, Ł.; Łukasiewicz, M. Synthesis and effect of structure on swelling properties of hydrogels based on high methylated pectin and acrylic polymers. *Polymers* **2019**, *11*, 114. [[CrossRef](#)]
40. Pourjavadi, A.; Barzegar, S. Synthesis and Evaluation of pH and Thermosensitive Pectin-Based Superabsorbent Hydrogel for Oral Drug Delivery Systems. *Starch-Stärke* **2009**, *61*, 161–172. [[CrossRef](#)]
41. Lan, Y.; Chen, B.; Rao, J. Pea protein isolate–high methoxyl pectin soluble complexes for improving pea protein functionality: Effect of pH, biopolymer ratio and concentrations. *Food Hydrocoll.* **2018**, *80*, 245–253. [[CrossRef](#)]
42. Namazi, H.; Rakhshaei, R.; Hamishehkar, H.; Kafil, H.S. Antibiotic loaded carboxymethylcellulose/MCM-41 nanocomposite hydrogel films as potential wound dressing. *Int. J. Biol. Macromol.* **2016**, *85*, 327–334. [[CrossRef](#)]
43. Ranjha, N.M.; Ayub, G.; Naseem, S.; Ansari, M.T. Preparation and characterization of hybrid pH-sensitive hydrogels of chitosan-co-acrylic acid for controlled release of verapamil. *J. Mater. Sci. Mater. Med.* **2010**, *21*, 2805–2816. [[CrossRef](#)]
44. Okudan, A.; Altay, A. Investigation of the effects of different hydrophilic and hydrophobic comonomers on the volume phase transition temperatures and thermal properties of N-isopropylacrylamide-based hydrogels. *Int. J. Polym. Sci.* **2019**, *2019*, 7324181. [[CrossRef](#)]
45. Rizwan, M.; Yahya, R.; Hassan, A.; Yar, M.; Azzahari, A.D.; Selvanathan, V.; Sonsudin, F.; Abouloula, C.N. pH sensitive hydrogels in drug delivery: Brief history, properties, swelling, and release mechanism, material selection and applications. *Polymers* **2017**, *9*, 137. [[CrossRef](#)]
46. Quintanilla de Stéfano, J.C.; Abundis-Correa, V.; Herrera-Flores, S.D.; Alvarez, A.J. PH-sensitive starch-based hydrogels: Synthesis and effect of molecular components on drug release behavior. *Polymers* **2020**, *12*, 1974. [[CrossRef](#)]
47. Folle, C.; Díaz-Garrido, N.; Sánchez-López, E.; Marqués, A.M.; Badia, J.; Baldomà, L.; Espina, M.; Calpena, A.C.; García, M.L. Surface-Modified Multifunctional Thymol-Loaded Biodegradable Nanoparticles for Topical Acne Treatment. *Pharmaceutics* **2021**, *13*, 1501. [[CrossRef](#)]
48. Limcharoen, B.; Pisetpackdeekul, P.; Toprangkobsin, P.; Thunyakitpisal, P.; Wanichwecharungruang, S.; Banlunara, W. Topical Preretinal Nanoparticles: Biological Activities, Epidermal Proliferation and Differentiation, Follicular Penetration, and Skin Tolerability. *ACS Biomater. Sci. Eng.* **2020**, *6*, 1510–1521. [[CrossRef](#)]
49. Bostanudin, M.F.; Lalatsa, A.; Górecki, D.C.; Barbu, E. Engineering butylglyceryl-modified polysaccharides towards nanomedicines for brain drug delivery. *Carbohydr. Polym.* **2020**, *236*, 116060. [[CrossRef](#)]
50. Salamanca, C.H.; Barrera-Ocampo, A.; Lasso, J.C.; Camacho, N.; Yarce, C.J. Franz diffusion cell approach for pre-formulation characterisation of ketoprofen semi-solid dosage forms. *Pharmaceutics* **2018**, *10*, 148. [[CrossRef](#)]
51. Haq, A.; Goodyear, B.; Ameen, D.; Joshi, V.; Michniak-Kohn, B. Strat-M®synthetic membrane: Permeability comparison to human cadaver skin. *Int. J. Pharm.* **2018**, *547*, 432–437. [[CrossRef](#)]
52. Vavrova, K.; Zbytovska, J.; Hrabalek, A. Amphiphilic Transdermal Permeation Enhancers: Structure-Activity Relationships. *Curr. Med. Chem.* **2005**, *12*, 2273–2291. [[CrossRef](#)] [[PubMed](#)]